Current Biology 20, 944–950, May 25, 2010 ©2010 Elsevier Ltd All rights reserved DOI 10.1016/j.cub.2010.03.068

Report

Cindr Interacts with Anillin to Control Cytokinesis in *Drosophila melanogaster*

Kaisa Haglund,[1,2,*] Ioannis P. Nezis,[1,2,6] Dafne Lemus,[1,2,6] Caroline Grabbe,[3] Jørgen Wesche,[1,2] Knut Liestøl,[2,4] Ivan Dikic,[5] Ruth Palmer,[3] and Harald Stenmark[1,2,*]

[1]Department of Biochemistry, Institute for Cancer Research, Oslo University Hospital, N-0310 Oslo, Norway
[2]Centre for Cancer Biomedicine, Faculty of Medicine, University of Oslo, Montebello, N-0310 Oslo, Norway
[3]Department of Molecular Biology, Umeå University, S-90187 Umeå, Sweden
[4]Department of Informatics, University of Oslo, N-0316 Oslo, Norway
[5]Institute of Biochemistry II, Frankfurt University Medical School, Theodor-Stein-Kai 7, D-60590 Frankfurt, Germany

Summary

Cytokinesis, the final step of cell division, conventionally proceeds to cell separation by abscission, or complete cytokinesis [1, 2], but may in certain tissues be incomplete, yielding daughter cells that are interconnected in syncytia by stable intercellular bridges [3]. The mechanisms that determine complete versus incomplete cytokinesis are not known. Here we report a novel in vivo role of the *Drosophila* CD2AP/CIN85 ortholog Cindr in both complete and incomplete cytokinesis. We also show evidence for the presence of persistent intercellular bridges in the major larval imaginal disc epithelia. During conventional division of both cultured and embryonic cells, Cindr localizes to cleavage furrows, intercellular bridges, and midbodies. Moreover, in cells undergoing incomplete cytokinesis in the female germline and the somatic ovarian follicle cell and larval imaginal disc epithelia, Cindr localizes to arrested cleavage furrows and stable intercellular bridges, respectively. In these structures, Cindr colocalizes with the essential cytokinesis regulator Anillin. We show that Cindr interacts with Anillin and that depletion of either Cindr or Anillin gives rise to binucleate cells and fewer intercellular bridges in vivo. We propose that Cindr and Anillin cooperate to promote intercellular bridge stability during incomplete cytokinesis in *Drosophila melanogaster*.

Results and Discussion

Cindr Colocalizes with Anillin and Regulates Cytokinesis in *Drosophila* S2 and Embryonic Cells

Because the in vivo functions of the evolutionarily conserved CD2AP (CD2-associated protein) and SH3KBP1 (SH3-domain kinase binding protein 1)/CIN85 (Cbl-interacting protein of 85 kDa) family of multiadaptor proteins remain incompletely understood, we set out to investigate the sole *Drosophila* CD2AP/CIN85 ortholog, Cindr (*CG31012*) (Figure S1A available online) [4]. We systematically analyzed Cindr expression and subcellular localization at various stages of *Drosophila* development and in cultured *Drosophila* S2 cells by using a Cindr antibody. One or both of the two largest Cindr isoforms were detected during oogenesis, embryogenesis, larval development, in adult flies, and in S2 cells by western blot (Figure 1B; Figure S1B) and immunocytochemistry (Figure 1A and see below).

In cultured *Drosophila* cells undergoing cytokinesis, Cindr localized to cleavage furrows, intercellular bridges, and the midbody (Figure 1A). After abscission, Cindr could further be detected in midbody remnants (Figure S1E). The essential cytokinesis regulator Anillin has previously been shown to localize in a similar manner during cell division ([5] and Figure S1F), so we analyzed its putative colocalization with Cindr, and indeed the two proteins colocalized throughout cytokinesis (Figure 1A). Cindr also colocalized with actin at the inner rim of the intercellular bridge (Figure S1G). To evaluate the functional importance of Cindr during cytokinesis, we studied the cellular phenotypes after Cindr depletion or overexpression. Effective reduction of *cindr* by RNA interference-mediated gene silencing (RNAi) resulted in an about 3-fold increase in the number of binucleate S2 cells, as compared to cells treated with control dsRNA (8.4% versus 2.6%, $p < 0.05$) (Figure 1B). During live imaging experiments, we observed that Cindr-depleted S2 cells displayed a delay in abscission and cleavage furrow regression in a similar cell percentage as above (Figure S1H, Table S1, and Movie S1 and data not shown). Consistently, overexpression of Cindr in human cells caused a dominant-negative effect, with a clear increase in the fraction of binucleate cells and cells in late cytokinesis (10% and 40%, respectively) as compared to control cells (3% and 10%, respectively) (Figure S1I).

Given the high expression of Cindr in *Drosophila* embryos (Figure S1B), we next investigated whether Cindr may be involved in conventional cell division during embryogenesis. In *Drosophila* embryonic mitotic domains [6], GFP-tagged endogenous Cindr colocalized with Anillin at contractile rings during early cytokinesis, as well as at midbodies during late cytokinesis (Figure S1J). Taken together, these data implicate a role for Cindr in cytokinesis during conventional cell divisions in cultured *Drosophila* cells and in the embryo.

Cindr Colocalizes with Anillin at Arrested Cleavage Furrows during Incomplete Cytokinesis in the *Drosophila* Female Germline

During oogenesis, we found Cindr expressed in both germ cells and the surrounding somatic follicle cell epithelium (Figures 2A, 2B, and 3A–3C; Figures S2A, S2B, and S3A–S3E and Movies S2 and S3). In germ cells, Cindr localized strongly to small ring-shaped structures in the anterior part of the germarium (Figures 2A and 2B), which is organized as follows (Figure S2A). In region 1, germ stem cell daughter cells, called cystoblasts, undergo four mitotic divisions by incomplete cytokinesis, leading to the formation of a cluster of 16 interconnected germ cells (Figure S2A) [7, 8]. The 16-cell cluster moves into region 2a, where the arrested cleavage furrows begin maturing into intercellular bridges called ring canals [9]. In order to determine the identity of the Cindr-postive rings, we

*Correspondence: stenmark@ulrik.uio.no (H.S.), kaisa.haglund@rr-research.no (K.H.)
[6]These authors contributed equally to this work

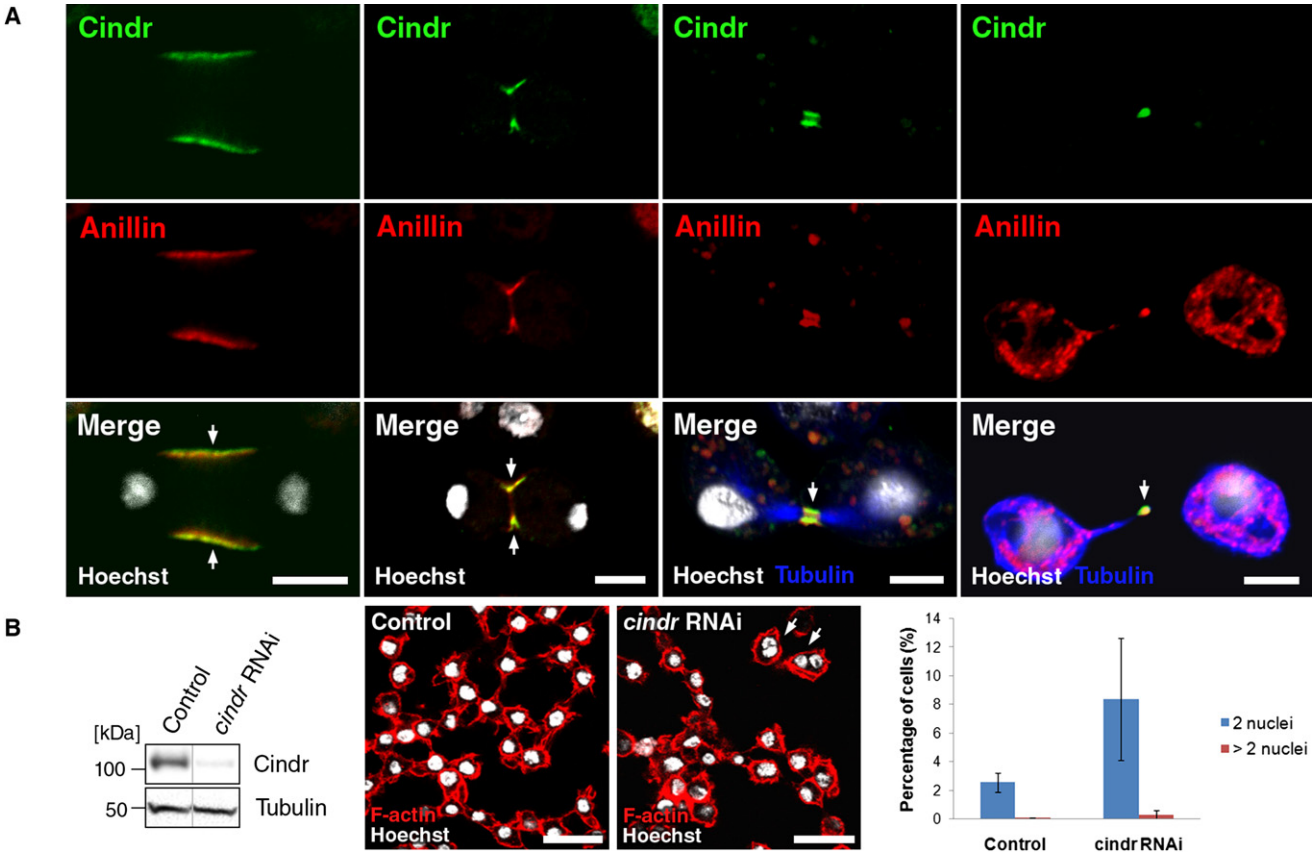

Figure 1. Cindr Colocalizes with Anillin and Regulates Cytokinesis in *Drosophila* S2 Cells

(A) Cindr colocalizes with Anillin during cytokinesis of *Drosophila* cells. Cindr and Anillin colocalize at cleavage furrows, intercellular bridges (ICBs), and midbodies of dividing S2 cells (arrows). Cells were fixed and stained with antibodies against Cindr (green), Anillin (red), α-tubulin (blue, the two panels at the right), and with Hoechst (white). Scale bars represent 5 μm.

(B) RNAi-mediated knockdown of Cindr causes binucleation of *Drosophila* cells. S2 cells were treated with control dsRNA (Control) or *cindr* dsRNAs 1+2 for 4 days (*cindr* RNAi). Left: Representative western blot showing reduced Cindr levels in *cindr* RNAi compared to control cells, which express the full-length Cindr isoform (Cindr-RC, 120 kDa). Its disappearance in *cindr* RNAi cells also confirms the Cindr antibody specificity. Levels of α-tubulin show equal protein loading. Middle: *cindr* RNAi cells display increased number of binucleate cells (arrows) compared to control cells. Cells were stained with rhodamine-phalloidin (red) and Hoechst (white). Scale bars represent 20 μm. Right: Graph showing the average percentage of bi- and multinucleate cells in control and *cindr* RNAi cells. Control, five independent experiments, n = 2901 cells; *cindr* RNAi, five independent experiments, n = 3269 cells. Data are presented as mean ± STD. Difference significant with $p < 0.05$. See also Figure S1 and Movie S1.

performed costainings with known cleavage furrow and ring canal components. We found that Cindr colocalized with Anillin (*CG2092*) and Pav-Klp (*CG1258*) [10, 11], two constituents of arrested cleavage furrows, in region 1 of the germarium (Figures S2A and S2B). In this area, Cindr localized strongly to cleavage furrows surrounding fusomes (Figure 2A; Movie S2), organelles that branch out in the germ cell cysts during the mitotic divisions [10]. Interestingly, in region 2a, upon fusome breakdown (Figure 2A; Movie S2) and recruitment of the ring canal markers hts-RC (*CG9325*) and phospho-tyrosine (pTyr) (Figure 2B) [12], Cindr disappeared from cleavage furrows. After this point we could not detect Cindr at growing ring canals during the rest of oogenesis (Figures 2A, 2B, 3A, and 3B; Figures S3A–S3C and S3E), which is interesting, because other known components remain for longer time (e.g., Anillin until stage 3; Pav-Klp, pTyr, and hts-RC throughout oogenesis) (Figure S2C). We therefore conclude that Cindr marks arrested cleavage furrows in mitotically active and newly formed germ cell clusters, but disappears from growing ring canals, suggesting a role in cleavage furrow formation and/or arrest, but not in ring canal growth.

Cindr Colocalizes with Anillin at Stable Somatic Intercellular Bridges in the *Drosophila* Egg Chamber Follicle Cell and Larval Imaginal Disc Epithelia

In *Drosophila*, each individual egg chamber is formed through encapsulation of the germ cells by an epithelium of somatic follicle cells, starting in region 2a of the germarium (Figure S2A and [7]). Interestingly, whereas Cindr disappeared from arrested cleavage furrows in the female germline, it abruptly appeared in dot-like structures in the forming egg chamber follicle cell epithelium in region 2a (Figures 2A and 2B; Figure S2B) and remained in such structures throughout oogenesis (Figures S3A and S3B). These were present throughout the follicle cell epithelium (Figure S3C and Movie S3) and consistently localized apically or at the level of the nuclei and at the borders between adjacent follicle cells (Figure 3A, left and middle images). They were localized basally of E-cadherin-containing adherens junctions (Figure 3A, right image) and did not overlap with markers for early (Rab5), late (Rab7), or recycling (Rab11 or Rab4) endosomes (Figure S3D). In light of the implication for Cindr in cytokinesis, we were interested to find reports describing incomplete cytokinesis in the follicle

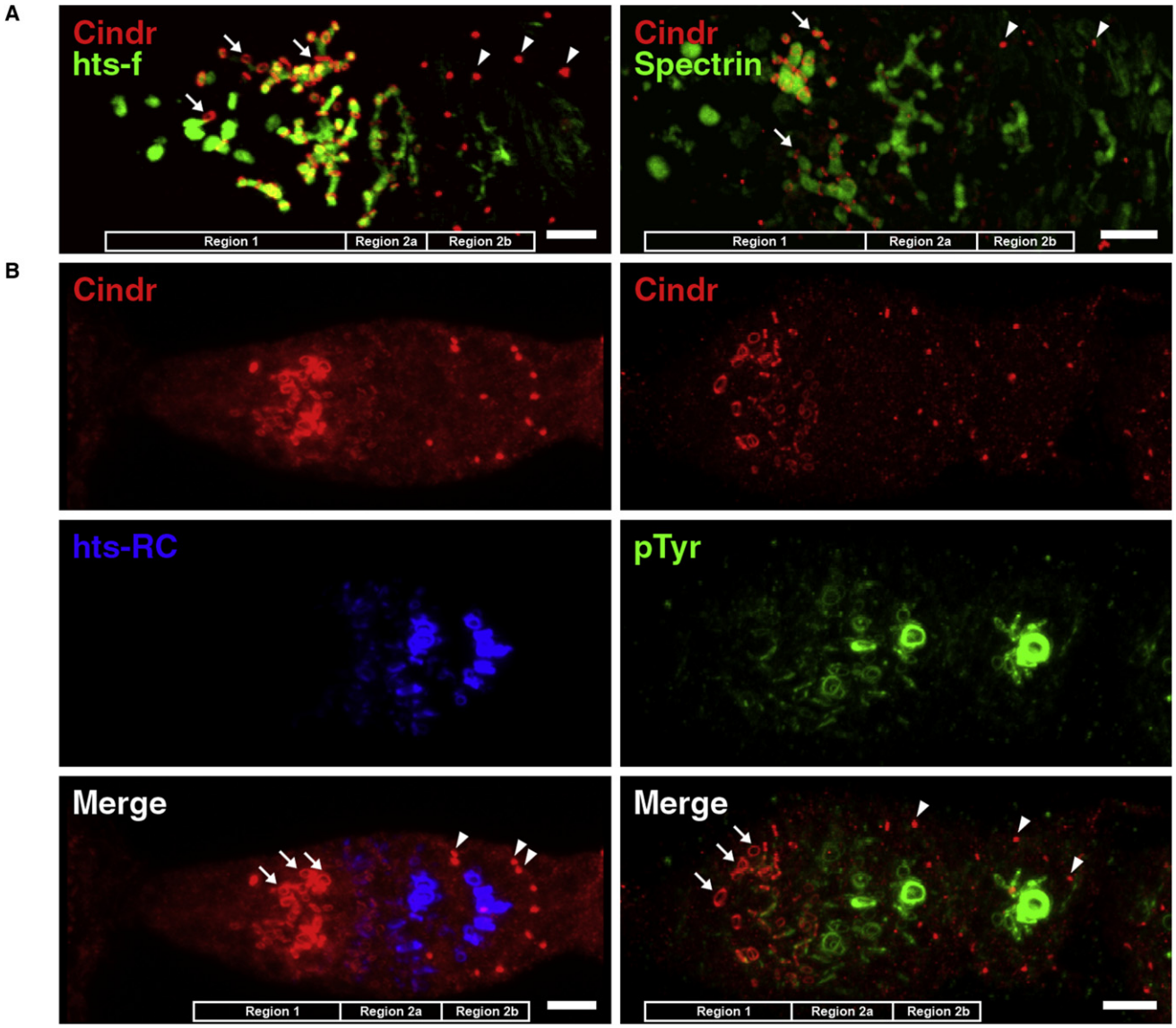

Figure 2. Cindr Localizes at Arrested Cleavage Furrows during Incomplete Cytokinesis in the *Drosophila* Female Germline

(A) Cindr (red) localizes to cleavage furrows (arrows) surrounding fusomes, labeled with hts-fusome (1B1, green, left image) or α-spectrin (green, right image), and gradually disappears as cell divisions cease in region 2a of the germarium. Subsequently, Cindr appears at ICBs (arrowheads) between the somatic cells of the forming follicle cell epithelium. The images are projections of z stacks of a whole germarium (left) or a part of one (right). Scale bars represent 5 μm.

(B) Cindr (red) localizes to arrested cleavage furrows (arrows) in region 1 of the germarium, but gradually disappears as the ring canal components hts-RC (blue; left panel) and phosphotyrosine (pY) epitopes (green, right panel) become localized in early region 2a and late region 1, respectively. Later, Cindr appears at ICBs between somatic follicle cells (arrowheads). The images are projections of z stacks of whole germaria. Scale bars represent 5 μm. See also Figure S2 and Movie S2.

cell epithelium, giving rise to follicle cell clusters with apically localized stable intercellular bridges [3, 13, 14]. Indeed, Cindr clearly colocalized with both Anillin and Pav-Klp, two known stable intercellular bridge components [10, 11], at intercellular bridges throughout oogenesis (Figure 3B; Figure S3E). Consistently, ultrastructural investigation by immunoelectron microscopy also demonstrated the presence of Cindr at follicle cell intercellular bridges, where it localized mainly at their inner rim in transverse, longitudinal, and oblique sections (Figure 3C).

Having identified Cindr at stable intercellular bridges during oogenesis, we next asked whether Cindr would be present at stable intercellular bridges during other stages of *Drosophila* development. For this purpose, we examined larval imaginal disc epithelia, out of which the wing and leg discs have previously been shown to contain stable intercellular bridges [3, 15, 16]. Indeed, Cindr localized to distinct structures present at cell borders that colocalized with Anillin throughout wing and leg discs (Figures 3D′, 3D″, 3E′, and 3E″; Movie S3) and was also detected in similar structures in eye and antennal discs (Figures 3F′, 3F″, 3G′, and 3G″; Figure S3F and Movie S3). These were confirmed to be intercellular bridges by electron microscopy (Figures 3D‴–3G‴) and were ultrastructurally similar to follicle cell intercellular bridges (Figure 3C and [14]). Cindr localized mainly to the inner rim also in wing disc

intercellular bridges (Figure 3D‴). These data indicate that all larval imaginal discs examined contain persistent intercellular bridges and that Cindr represents a stable intercellular bridge component during *Drosophila* development.

Additionally, also in the larval brain, we found that Cindr localized at structures present at cell borders (Figure 3H′; Movie S3) that colocalized with Anillin (Figure 3H″) and bridges displaying the characteristic intercellular bridge ultrastructure (Figure 3H‴). Indeed, the larval brain has been suggested to contain stable intercellular bridges [15], but this remains an area of investigation. Interestingly, intercellular bridges of dividing neuroblasts displayed a more variable morphology (Figure S3G). Consistent with the data in Figures 1 and 2, Cindr moreover localized to contractile rings in the larval imaginal discs and brain (Figures S3H and S3I).

Cindr Regulates Intercellular Bridge Stability In Vivo and Interacts with Anillin

We next examined the role of Cindr at stable intercellular bridges in vivo. RNAi-mediated *cindr* depletion in somatic follicle cells resulted in a significant increase in the number of binucleate cells (~10%), as compared to control egg chambers, which contained essentially only mononucleate cells (Figures 4A and 4B; Figure S4A). Similarly, RNAi-mediated knockdown of *anillin* dramatically increased the number of binucleate follicle cells (~40%) (Figures 4A and 4B). Interestingly, the increase in binucleate cells was accompanied by a significant decrease in the average number of follicle cell intercellular bridges per nucleus (cindr, $p < 0.05$; anillin, $p < 0.01$) (Figure 4C), whereas the number of bridges compared to the number of cells was essentially unchanged (Figure S4B). The higher levels of binucleate cells in Anillin- compared to Cindr-depleted epithelia may be accounted for by a faster depletion of Anillin compared to Cindr protein levels. In Anillin-depleted epithelia, we indeed detected binucleate follicle cells in early egg chamber stages arising from defective cell divisions (Figure S4C), whereas binucleate Cindr-depleted cells were detected only at late egg chamber stages (Figure 4A; Figures S4A and S4C) after the cease of follicle cell divisions in stage 6. These findings indicate a role for Cindr in stabilizing intercellular bridges in the follicle epithelium during oocyte growth.

To address the molecular mechanisms by which Cindr may act at intercellular bridges, we finally asked whether Cindr and Anillin may interact, given their similar localization pattern throughout *Drosophila* development and the presence of a Px(P/A)xxR motif (**PLARLR**, amino acids 145–150) in Anillin (Figure 4D). Such motifs interact with the SH3 domains of mammalian CD2AP/CIN85 family members [17, 18] and in fact CD2AP interacts with such a motif in human Anillin [19]. The SH3 domains of Cindr show high sequence homology with the SH3 domains of CD2AP/CIN85 (Figure S1A), and in pull-down experiments via four GST-tagged parts of Anillin, Cindr indeed associated with the most N-terminal (GST-A1) **PLARLR**-containing region of Anillin (Figure 4D). Importantly, mutation of the consensus arginine to alanine (R150A) in the motif abolished the interaction with Cindr (Figure 4D). We also detected an interaction between Cindr and the C-terminal (GST-A4) region of Anillin (Figure 4D), which is interesting because CD2AP and human Anillin were reported to associate only via an N-terminal Px(P/A)xxR motif [19]. Taken together, these data indicate that Cindr interacts with *Drosophila* Anillin via two distinct sites: the **PLARLR** motif via its SH3 domains and an additional site in the C terminus of Anillin.

In summary, we have identified a novel in vivo role of Cindr as a general component of stable intercellular bridges during *Drosophila* development. Cindr localizes to arrested cleavage furrows in the female germline and to somatic stable intercellular bridges in the follicle cell and larval imaginal disc epithelia. Only a limited number of such components have previously been described, including Anillin, Pav-Klp, and Mucin-D [9–11, 15], and interestingly Cindr interacts with Anillin and colocalizes with it at intercellular bridges throughout *Drosophila* development. Given the increase in binucleate cells and decrease in intercellular bridge numbers upon Cindr and Anillin depletions in follicle cells, we propose that Cindr and Anillin interact to promote intercellular bridge stability in tissues that undergo incomplete cytokinesis. One mechanism may be via stabilization of actin at the inner rim of the bridge [9, 20], as indicated by the fact that Cindr/CD2AP/CIN85 and Anillin are well-established actin regulators [4, 21–23] and Cindr indeed localizes to the inner rim of stable follicle cell intercellular bridges that is lined with actin filaments [14] (Figure 4E). During conventional cell divisions, Cindr and Anillin may play a similar role [24], as shown by the fact that Cindr colocalizes with actin in the bridge, and we also find Cindr participating in the final abscission step, like CD2AP [19]. We note that the CD2AP/CIN85/Cindr family of proteins may function as scaffold proteins during cytokinesis because of their ability to oligomerize [25] and to associate with Anillin, and possibly septins, MgcRacGAP/RacGAP50C, and MKLP1/Pav-Klp [19, 26]. Finally, we show the presence of persistent intercellular bridges in the major larval imaginal disc epithelia, suggesting that their development may require coordinated intercellular communication within cellular syncytia. A better understanding of complete and incomplete cytokinesis in vivo, to which our data contribute, not only expands the knowledge about these processes during development, but may also provide clues to how accurate cytokinesis regulation is achieved to prevent cell division defects associated with cancer development.

Experimental Procedures

Drosophila melanogaster Strains

Fly crosses and experiments were performed at 25°C unless noted otherwise. The following stocks were used: w^{1118} and *MS1096-GAL4* (from Bloomington *Drosophila* Stock Center at Indiana University, http://flystocks.bio.indiana.edu/); *cindr-IR*$^{2.21+23,3.63+76}$ (gift from R. Johnson and R. Cagan, Mount Sinai Medical School, New York, NY) [4]; *GFP trap CA06686* (*CG31012* Cindr isoform C) and *GFP trap CA06810* (*CG31012* Cindr isoforms C and D) (from FlyTrap GFP Protein Trap Database, http://flytrap.med.yale.edu/) [27]; *UAS-anillin-IR* (chr 3) (from VDRC, http://www.vdrc.at) [28]; *UAS-Venus-anillin* (chr 3) (gift from R. Saint, The University of Adelaide, Adelaide, Australia) [29]; *GR1-GAL4/TM3, Sb* (gift from N. Denef and T. Schupbach, Princeton University, Princeton, NJ); *GR1-GAL4, UAS-dsRed (nls)/TM3, Sb* (recombined to *UAS-dsRed (nls)* [gift from T.P. Neufeld, University of Minnesota, Minneapolis, MN]), w^{1118}*; p[w+ Ub-GFP-Pav-KLP]53* (chr 2) (gift from D. Glover, University of Cambridge, Cambridge, UK) [11]; and *rab5-YFP, rab7-YFP, rab11-YFP*, and *rab4-YFP* (gifts from S. Eaton, Max Planck Institute of Molecular Cell Biology and Genetics, Dresden, Germany) [30].

RNAi-Mediated Knockdown In Vivo

For RNAi-mediated knockdown in follicle cells, *GR1-GAL4, UAS-dsRed/TM3, Sb* males were crossed to *UAS-cindr-IR*$^{2.21+23,3.63+76}$, *UAS-anillin-IR* or w^{1118} female virgins. Crosses were kept at 18°C to allow viability of *UAS-cindr-IR*$^{3.63+76}$*/+; GR1-GAL4, UAS-dsRed/UAS-cindr-IR*$^{2.21+23}$ offspring. 2-day-old adult females of genotypes *UAS-cindr-IR*$^{3.63+76}$*/+; GR1-GAL4, UAS-dsRed/UAS-cindr-IR*$^{2.21+23}$*, GR1-GAL4, UAS-dsRed/UAS-anillin-IR* or *GR1-GAL4, UAS-dsRed/+* were shifted to 25°C for 24 hr and then to 29°C for 48 hr to allow expression of RNAi in the follicle cells. At the same time, oogenesis was stimulated by addition of yeast paste

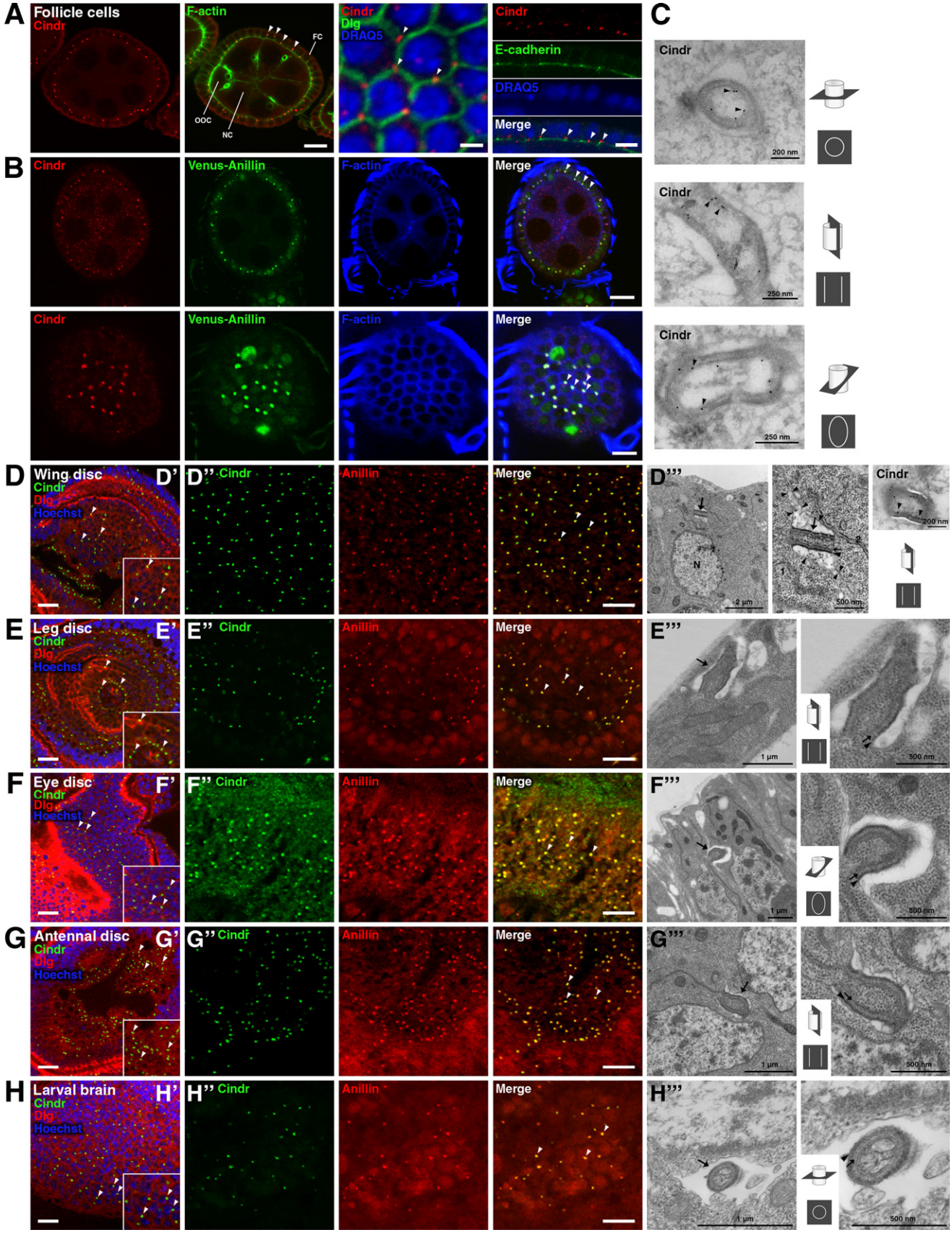
A
Follicle cells
Cindr
F-actin
FC
OOC
NC
Cindr
Dlg
DRAQ5
Cindr
E-cadherin
DRAQ5
Merge
B
Cindr
Venus-Anillin
F-actin
Merge
Cindr
Venus-Anillin
F-actin
Merge
C
Cindr
200 nm
Cindr
250 nm
Cindr
250 nm
D
Wing disc
D'
Cindr
Dlg
Hoechst
D'' Cindr
Anillin
Merge
D'''
N
2 µm
1
2
500 nm
Cindr
200 nm
E
Leg disc
E'
Cindr
Dlg
Hoechst
E'' Cindr
Anillin
Merge
E'''
1 µm
500 nm
F
Eye disc
F'
Cindr
Dlg
Hoechst
F'' Cindr
Anillin
Merge
F'''
1 µm
500 nm
G
Antennal disc
G'
Cindr
Dlg
Hoechst
G'' Cindr
Anillin
Merge
G'''
1 µm
500 nm
H
Larval brain
H'
Cindr
Dlg
Hoechst
H'' Cindr
Anillin
Merge
H'''
1 µm
500 nm

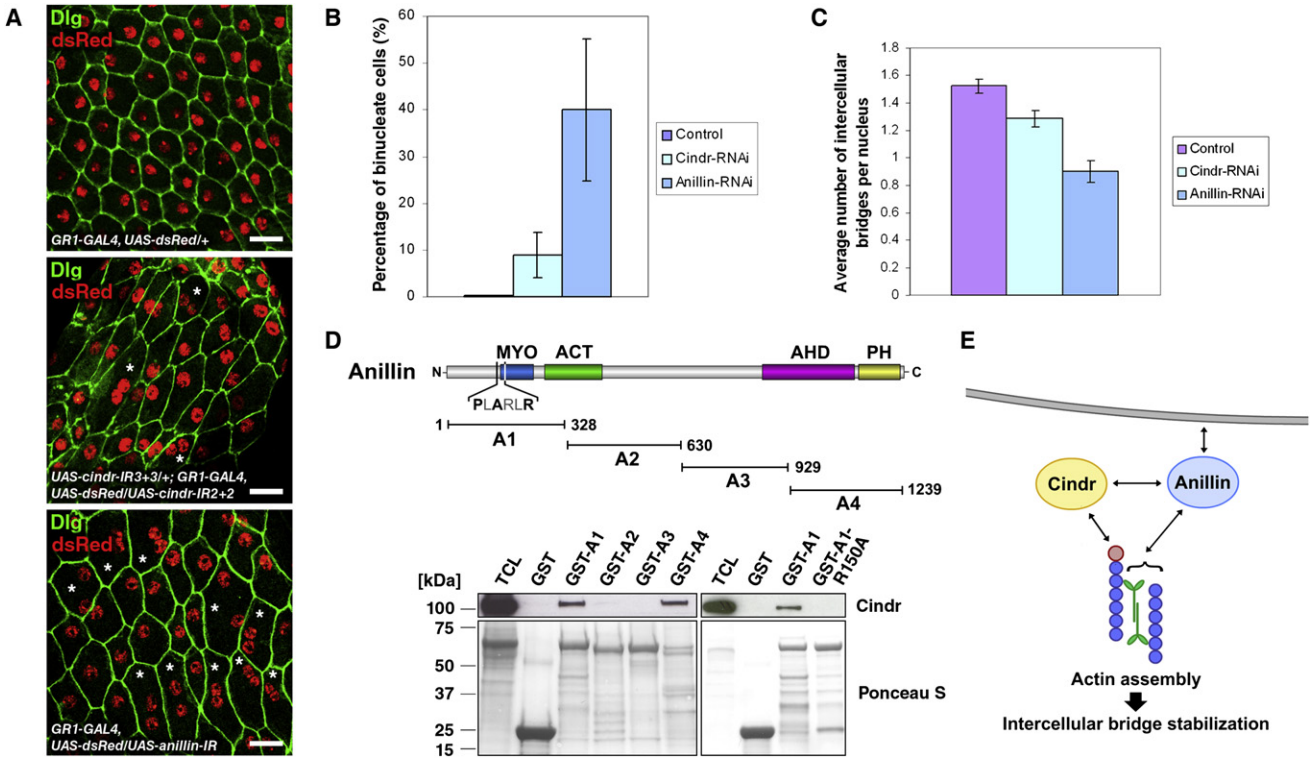

Figure 4. Cindr Regulates Intercellular Bridge Stability In Vivo and Interacts with Anillin

(A) Cindr and Anillin depletions in the follicle cell epithelium give rise to binucleate cells (asterisks). Top: Control egg chamber follicle cell epithelium expressing dsRed. *Cindr* (middle) or *anillin* (bottom) RNAi were expressed in the follicle cell epithelium via the *GR1-GAL4, UAS-dsRed (nls)* driver (red) as described in the Experimental Procedures. Ovaries were fixed and stained with anti-Dlg (green). Scale bars represent 20 μm.

(B) Graph showing the average percentage of binucleate follicle cells for each genotype in (A). Control, three independent experiments, n = 1838 cells, 14 egg chambers from more than 10 flies; *cindr* RNAi, three independent experiments, n = 1638 cells, 25 egg chambers from more than 20 flies; *anillin* RNAi, three independent experiments, n = 2138 cells, 23 egg chambers from more than 20 flies. Data are presented as mean ± STD. See also Figure S4A.

(C) Graph showing the average number of ICBs per follicle cell nucleus for each genotype in (A). Experiments were performed as described in the Supplemental Experimental Procedures. Control, three independent experiments, n = 480 nuclei from more than 20 egg chambers and 15 individual flies; *cindr* RNAi, three independent experiments, n = 600 nuclei from more than 20 egg chambers and 15 individual flies; *anillin* RNAi, three independent experiments, n = 340 nuclei from more than 15 egg chambers and 12 individual flies. Data are presented as mean ± STD. See also Figure S4B.

(D) Cindr interacts with Anillin. Top: *Drosophila* Anillin and the GST-Anillin fragments (A1, A2, A3, and A4) used for the GST pulldown experiment with their respective lengths in amino acids. MYO, myosin-binding region; ACT, actin-binding region; AHD, Anillin homology domain; PH, pleckstrin homology domain. A (**P**)x(**P**/**A**)xx(**R**) consensus motif (**P**)L(**A**)RL(**R**) (amino acids 145–150) is present in the N-terminal part of Anillin. Bottom: Cindr interacts with GST-A1 and A4, but not A2 and A3. The R150A mutation in the (**P**)L(**A**)RL(**R**) motif in GST-A1 abolishes the interaction. Ponceau S staining shows the levels of GST (negative control) and GST fusion proteins. TCL, total cell lysate, 10% of input.

(E) Model of proposed action of Cindr and Anillin at intercellular bridges (ICBs). Cindr and Anillin may cooperate to promote ICB stabilization by actin assembly at the ICB inner rim by interactions with F-actin (blue) and actin regulators (red, e.g., F-actin capping protein Cpb [4]).

Figure 3. Cindr Colocalizes with Anillin at Stable Somatic Intercellular Bridges in the *Drosophila* Egg Chamber Follicle Cell and Larval Imaginal Disc Epithelia

(A) Cindr (red) localizes to follicle cell ICBs (arrowheads). Left two images: Cindr localizes apically to or at the level of the nucleus in the follicle cell epithelium. Scale bar represents 10 μm. OOC, oocyte; NC, nurse cells; FC, follicle cells. Third image: Cindr-positive (red) ICBs are found at follicle cell borders, outlined by Dlg (green). Scale bar represents 2 μm. Right image: Cindr (red) localizes in close proximity to, but does not overlap with, E-cadherin-containing adherens junctions (green). Scale bar represents 5 μm.

(B) Cindr (red) colocalizes with Anillin (green) at follicle cell ICBs (arrowheads). Venus-tagged Anillin (green) was expressed in follicle cells via the *GR1-GAL4* driver. Egg chambers were fixed and stained with anti-Cindr (red) and phalloidin (blue). Top panels: Cross section through a stage 8 egg chamber. Scale bar represents 10 μm. Bottom panels: A superficial apical section through the follicle cell epithelium. Scale bar represents 5 μm.

(C) Immunoelectron micrographs showing Cindr (gold particles, arrowheads) localization mainly to the inner rim of follicle cell ICBs in transverse (top), longitudinal (middle), and oblique (bottom) sections. Scale bars represent 200 nm (top) and 250 nm (middle and bottom).

(D–H) Cindr (green, arrowheads) localizes at cell borders, outlined by Dlg (red), in larval wing (D′), leg (E′), eye (F′), and antennal (G′) imaginal discs, and brain (H′). Scale bars represent 10 μm.

(D″–H″) Cindr (green) colocalizes with Anillin (red) at ICBs (arrowheads) throughout wing disc (D″), leg disc (E″), the anterior part of the eye disc (F″), and throughout antennal disc epithelia (G″), and in the outer part of the larval brain (H″). Wild-type wing, leg, and antennal discs and larval brain were stained with Cindr (green) and Anillin (red) antibodies (D″, E″, G″, H″) or GFP trap CA06686 (*Cindr isoform C*) larval eye discs with anti-GFP (green) and anti-Anillin (red) (F″). Scale bars represent 10 μm.

(D‴–H‴) Left: Electron micrographs of ICBs (arrows) in wing (D‴) (N, nucleus), leg (E‴), eye (F‴), antennal (G‴) disc epithelia and the larval brain (H‴). Scale bars represent 2 μm (D‴) and 1 μm (E‴–H‴). Middle (D‴): The wing disc ICB (big arrow) diameter is about 0.3 μm and its wall consists of an electron-dense outer rim (big arrowhead) and an inner rim (small arrow). Small arrowheads outline the plasma membrane of the two interconnected cells (1 and 2). Scale bar represents 500 nm. Right (D‴): Immunoelectron micrograph indicating Cindr (gold particles, arrowheads) localization mainly to the inner rim of a wing disc ICB. Scale bar represents 200 nm. Right (E‴–H‴): Magnifications of ICBs in leg (E‴), eye (F‴), and antennal (G‴) disc epithelia and in the larval brain (H‴) in which the outer (arrowheads) and inner (arrows) rims are evident. Scale bars represent 500 nm. See also Figure S3 and Movie S3.

and a couple of males. Ovaries were dissected, fixed, and stained with anti-Dlg (1:100).

For additional methods, please refer to the Supplemental Experimental Procedures.

Supplemental Information

Supplemental Information includes Supplemental Experimental Procedures, four figures, one table, and three movies and can be found with this article online at doi:10.1016/j.cub.2010.03.068.

Acknowledgments

We are grateful to Ruth Johnson, Ross Cagan, David Glover, Pier Paolo d'Avino, Natalie Denef, Trudi Schupbach, Suzanne Eaton, Robert Saint, Ronald D. Vale, Eric Griffis, Stephen Gregory, Michael Zavortink, Maria Giovanna Riparbelli, Terje Johansen, Thomas P. Neufeld, and Tor Erik Rusten for fly lines, constructs, antibodies, and helpful suggestions. We also thank members of our laboratories for valuable discussions. K.H. acknowledges a postdoctoral fellowship from the International Human Frontier Science Program Organization. She currently holds a senior scientist grant from the Research Council of Norway. I.P.N. is a postdoctoral fellow of the Research Council of Norway. D.L. is a predoctoral fellow of the South-Eastern Norway Regional Health Authority. J.W. is a senior research fellow of the Norwegian Cancer Society. H.S. acknowledges an Advanced Grant from the European Research Council.

Received: August 13, 2009
Revised: March 29, 2010
Accepted: March 29, 2010
Published online: May 6, 2010

References

1. Eggert, U.S., Mitchison, T.J., and Field, C.M. (2006). Animal cytokinesis: From parts list to mechanisms. Annu. Rev. Biochem. *75*, 543–566.
2. Barr, F.A., and Gruneberg, U. (2007). Cytokinesis: Placing and making the final cut. Cell *131*, 847–860.
3. Robinson, D.N., and Cooley, L. (1996). Stable intercellular bridges in development: The cytoskeleton lining the tunnel. Trends Cell Biol. *6*, 474–479.
4. Johnson, R.I., Seppa, M.J., and Cagan, R.L. (2008). The *Drosophila* CD2AP/CIN85 orthologue Cindr regulates junctions and cytoskeleton dynamics during tissue patterning. J. Cell Biol. *180*, 1191–1204.
5. D'Avino, P.P., Takeda, T., Capalbo, L., Zhang, W., Lilley, K.S., Laue, E.D., and Glover, D.M. (2008). Interaction between Anillin and RacGAP50C connects the actomyosin contractile ring with spindle microtubules at the cell division site. J. Cell Sci. *121*, 1151–1158.
6. Foe, V.E. (1989). Mitotic domains reveal early commitment of cells in *Drosophila* embryos. Development *107*, 1–22.
7. Horne-Badovinac, S., and Bilder, D. (2005). Mass transit: Epithelial morphogenesis in the *Drosophila* egg chamber. Dev. Dyn. *232*, 559–574.
8. Pepling, M.E., de Cuevas, M., and Spradling, A.C. (1999). Germline cysts: A conserved phase of germ cell development? Trends Cell Biol. *9*, 257–262.
9. Robinson, D.N., and Cooley, L. (1997). Genetic analysis of the actin cytoskeleton in the *Drosophila* ovary. Annu. Rev. Cell Dev. Biol. *13*, 147–170.
10. de Cuevas, M., and Spradling, A.C. (1998). Morphogenesis of the *Drosophila* fusome and its implications for oocyte specification. Development *125*, 2781–2789.
11. Minestrini, G., Mathe, E., and Glover, D.M. (2002). Domains of the Pavarotti kinesin-like protein that direct its subcellular distribution: Effects of mislocalisation on the tubulin and actin cytoskeleton during *Drosophila* oogenesis. J. Cell Sci. *115*, 725–736.
12. Robinson, D.N., Cant, K., and Cooley, L. (1994). Morphogenesis of *Drosophila* ovarian ring canals. Development *120*, 2015–2025.
13. Giorgi, F. (1978). Intercellular bridges in ovarian follicle cells of *Drosophila melanogaster*. Cell Tissue Res. *186*, 413–422.
14. Woodruff, R.I., and Tilney, L.G. (1998). Intercellular bridges between epithelial cells in the *Drosophila* ovarian follicle: A possible aid to localized signaling. Dev. Biol. *200*, 82–91.
15. Kramerova, I.A., and Kramerov, A.A. (1999). Mucinoprotein is a universal constituent of stable intercellular bridges in *Drosophila melanogaster* germ line and somatic cells. Dev. Dyn. *216*, 349–360.
16. Poodry, C.A., and Schneiderman, H.A. (1970). Ultrastructure of the developing leg of *Drosophila melanogaster*. Wilhelm Roux Archiv. *166*, 1–44.
17. Kowanetz, K., Szymkiewicz, I., Haglund, K., Kowanetz, M., Husnjak, K., Taylor, J.D., Soubeyran, P., Engstrom, U., Ladbury, J.E., and Dikic, I. (2003). Identification of a novel proline-arginine motif involved in CIN85-dependent clustering of Cbl and down-regulation of epidermal growth factor receptors. J. Biol. Chem. *278*, 39735–39746.
18. Kurakin, A.V., Wu, S., and Bredesen, D.E. (2003). Atypical recognition consensus of CIN85/SETA/Ruk SH3 domains revealed by target-assisted iterative screening. J. Biol. Chem. *278*, 34102–34109.
19. Monzo, P., Gauthier, N.C., Keslair, F., Loubat, A., Field, C.M., Le March-and-Brustel, Y., and Cormont, M. (2005). Clues to CD2-associated protein involvement in cytokinesis. Mol. Biol. Cell *16*, 2891–2902.
20. Steigemann, P., Wurzenberger, C., Schmitz, M.H., Held, M., Guizetti, J., Maar, S., and Gerlich, D.W. (2009). Aurora B-mediated abscission checkpoint protects against tetraploidization. Cell *136*, 473–484.
21. Gaidos, G., Soni, S., Oswald, D.J., Toselli, P.A., and Kirsch, K.H. (2007). Structure and function analysis of the CMS/CIN85 protein family identifies actin-bundling properties and heterotypic-complex formation. J. Cell Sci. *120*, 2366–2377.
22. Welsch, T., Endlich, N., Gokce, G., Doroshenko, E., Simpson, J.C., Kriz, W., Shaw, A.S., and Endlich, K. (2005). Association of CD2AP with dynamic actin on vesicles in podocytes. Am. J. Physiol. Renal Physiol. *289*, F1134–F1143.
23. D'Avino, P. (2009). How to scaffold the contractile ring for a safe cytokinesis—Lessons from Anillin-related proteins. J. Cell Sci. *122*, 1071–1079.
24. Echard, A., Hickson, G.R., Foley, E., and O'Farrell, P.H. (2004). Terminal cytokinesis events uncovered after an RNAi screen. Curr. Biol. *14*, 1685–1693.
25. Dikic, I. (2002). CIN85/CMS family of adaptor molecules. FEBS Lett. *529*, 110–115.
26. Havrylov, S., Rzhepetskyy, Y., Malinowska, A., Drobot, L., and Redowicz, M.J. (2009). Proteins recruited by SH3 domains of Ruk/CIN85 adaptor identified by LC-MS/MS. Proteome Sci. *7*, 21.
27. Buszczak, M., Paterno, S., Lighthouse, D., Bachman, J., Planck, J., Owen, S., Skora, A.D., Nystul, T.G., Ohlstein, B., Allen, A., et al. (2007). The carnegie protein trap library: A versatile tool for *Drosophila* developmental studies. Genetics *175*, 1505–1531.
28. Dietzl, G., Chen, D., Schnorrer, F., Su, K.C., Barinova, Y., Fellner, M., Gasser, B., Kinsey, K., Oppel, S., Scheiblauer, S., et al. (2007). A genome-wide transgenic RNAi library for conditional gene inactivation in *Drosophila*. Nature *448*, 151–156.
29. Gregory, S.L., Ebrahimi, S., Milverton, J., Jones, W.M., Bejsovec, A., and Saint, R. (2008). Cell division requires a direct link between microtubule-bound RacGAP and Anillin in the contractile ring. Curr. Biol. *18*, 25–29.
30. Marois, E., Mahmoud, A., and Eaton, S. (2006). The endocytic pathway and formation of the Wingless morphogen gradient. Development *133*, 307–317.